

Role of anharmonicities and non-linearities in heavy ion collisions. A microscopic approach.

E.G. Lanza^a, M.V. Andrés^b, F. Catara^a, Ph. Chomaz^c and C. Volpe^c

^a *Dipartimento di Fisica Università di Catania and INFN, Sezione di Catania, I-95129 Catania, Italy*

^b *Departamento de Física Atómica, Molecular y Nuclear, Universidad de Sevilla, Apdo 1065, 41080 Sevilla, Spain*

^c *GANIL, B.P. 5027, F-14021 Caen Cedex, France*

Abstract: Using a microscopic approach beyond RPA to treat anharmonicities, we mix two-phonon states among themselves and with one-phonon states. We also introduce non-linear terms in the external field. These non-linear terms and the anharmonicities are not taken into account in the "standard" multiphonon picture. Within this framework we calculate Coulomb excitation of ^{208}Pb and ^{40}Ca by a ^{208}Pb nucleus at 641 and 1000 MeV/A. We show with different examples the importance of the non-linearities and anharmonicities for the excitation cross section. We find an increase of 10% for ^{208}Pb and 20% for ^{40}Ca of the excitation cross section corresponding to the energy region of the double giant dipole resonance with respect to the "standard" calculation. We also find important effects in the low energy region. The predicted cross section in the DGDR region is found to be rather close to the experimental observation.

1 Introduction

States that can be interpreted as the first quanta of collective vibrations are a general property of quantum mesoscopic systems which can be found in various fields of physics. In nuclear physics, such vibrational states of the nucleus have been known for many years [1]. These one-phonon states are present both in the low-lying excitation spectra of nuclei and at higher energies. The latter are the Giant Resonances (GR). The existence of two-phonon states, i.e. states

which can be described as double excitations of elementary modes, has also been predicted since the early days of the collective model [1]. Such states have been observed long time ago in the low-lying spectra. More recently, two-phonon states built with giant resonances have been populated in heavy ion inelastic scattering [2], in double charge exchange (π^\pm, π^\mp) reactions [3] and in Coulomb excitation at high energy [4–6]. For a review, see ref. [7].

In the harmonic approximation, these states are predicted as degenerate multiplets located at an excitation energy equal to the sum of the individual phonon energies. When the residual interaction is taken into account, the degeneracy is broken by the coupling between phonons. In the present article we consider the residual interaction of two-phonon states among themselves and with one-phonon states. Therefore, the eigenstates are linear combinations of one- and two-phonon components while the energies are shifted and splitted with respect to the harmonic limit. We will call such states mixed states. Evidence of such anharmonic behaviour can be found, for example, in a (γ, γ') experiment [8] where the observation of large dipole strength in the low-lying spectrum of some Sn isotopes is reported. Such strength is interpreted by the authors as due partially to the population of the 1^- member of the quintuplet of states based on the $|2^+ \otimes 3^- \rangle$ two-phonon state, and partially to the admixture of the (one-phonon) GDR in the wavefunction of the state observed around 3.5 MeV excitation energy. As it has been shown in [9], the inclusion of the residual interaction among two-phonon states leads to small, but sizeable, anharmonicities also in the high-lying spectrum, namely for those states that in the harmonic limit are described as double excitations of GR. The mixing between one- and two-phonon states further increases the anharmonicities. When an external field acts on a nucleus, it excites the eigenstates of the internal hamiltonian, which, in our approach, are superpositions of one- and two-phonon states.

The microscopic theory suited for the description of collective vibrational states is the Random Phase Approximation (RPA). Two-phonon states and their mixing among themselves and with one-phonon states can be generated by using boson mapping techniques and by taking into account terms of the residual interaction which do not enter at the RPA level [9,10]. In this way one has an RPA based approach to treat anharmonicities.

In a nucleus-nucleus collision, the mutual excitation of the two partners is described as due to the action of the mean field of each nucleus on the other one, i.e. by a one body operator. Assuming that it induces small deformations of the density, only the particle-hole (ph) terms of the external mean field are usually taken into account. This amounts to consider as elementary processes only those corresponding to the creation or annihilation of one phonon. In this approximation, the external field is linear in the creation and annihilation operators of phonons. When the particle-particle (pp) and hole-hole (hh) terms

of the external field are also included, the direct excitation from the ground state to two-phonon states as well as the transition between one-phonon states become possible. These terms can be expressed as quadratic in the creation and annihilation operators of phonons and so correspond to non-linear terms in the excitation operator.

In the "standard" approach, based on the independent multiphonon picture, the effects coming from both anharmonicities and non-linearities are neglected (see for instance ref.[11]). Recent experimental data on Coulomb excitation at relativistic energies have raised some questions on the adequacy of that picture. Indeed, in the excitation of ^{136}Xe on ^{208}Pb , the experimental cross section to the double GDR (DGDR) has been found to be 2 to 4 times larger than the theoretical one [4]. Recently, new experimental results [6] on the excitation of several nuclei have shown that the disagreement ranges from about 10% to 60%, being about 30% in the case of ^{208}Pb . In a previous paper [12], by using a one-dimensional oscillator model to mimic nuclear states, we have shown that the effects of anharmonicities and non-linearities can lead to an important enhancement of the cross section in the energy range around twice that of the GDR. In this model neither spin nor parity were taken into account. Besides, only one type of phonons was considered. In the present paper we present more realistic calculations, where the collective states of the target nucleus and the action on it of the Coulomb field of the projectile are described starting from RPA. Anharmonicities and non-linearities are included by means of boson mapping techniques. Both low-lying collective states and giant resonances are considered as elementary phonons.

We have done calculations for the $^{208}\text{Pb}+^{208}\text{Pb}$ system at 641 and 1000 MeV per nucleon for which experimental data exist [6]. We have also studied the Coulomb excitation of ^{40}Ca in the reaction $^{208}\text{Pb}+^{40}\text{Ca}$ at 1000 MeV/A although there are no experimental data for this case. In both cases we consider as elementary modes all natural-parity RPA phonons whose multipolarity is lower than 4 and whose contribution to the associated energy weighted sum rule (EWSR) is larger than 5%. Then, we have built the residual interaction in the one and two-phonon space and we have diagonalized the hamiltonian in this subspace in order to define the mixed states $|\phi_\alpha\rangle$. By solving the time dependent Schrödinger equation in this subspace we get the probability amplitudes for each of the $|\phi_\alpha\rangle$ states from which we calculate the cross section. We will describe in detail the results for the $^{208}\text{Pb}+^{208}\text{Pb}$ system at 641 MeV/A, the results at 1000 MeV/A being essentially the same except for the absolute values of the cross section which are higher in the latter case. We will mostly discuss the two regions around the energy of the states built with two low-lying states or with two giant resonances. We will see that non-linearities and anharmonicities may strongly change the cross sections associated with some specific states. Their influence is found to be of the order of 10% for ^{208}Pb and 20% for ^{40}Ca in the DGDR energy region, bringing the theoretical

results closer to the experimental ones.

In the next section we detail the model employed and in section 3 we describe the semiclassical electromagnetic field used to excite the nuclei. Section 4 is devoted to the description of the results on ^{208}Pb where we discuss in a detailed way the effects of both anharmonicities and non-linear terms on the excitation cross section. The results for ^{40}Ca are reported in section 5 and finally we draw our conclusions in section 6.

2 The multiphonon picture

Heavy ion collisions at high incident energies can be described within a semiclassical approach, where the relative motion is treated classically while quantum mechanics is used for the internal degrees of freedom of the colliding nuclei. For grazing and large impact parameter collisions the densities of the two nuclei have a small overlap. Therefore, the total hamiltonian can be written as

$$H = H_A + H_B \quad (1)$$

where $H_A(H_B)$ denotes the hamiltonian of nucleus A(B) and

$$H_A = H_A^0 + \sum_{\alpha\alpha'} \langle \alpha | U_B(\mathbf{R}(t)) | \alpha' \rangle a_\alpha^\dagger a_{\alpha'} = H_A^0 + W_A(t) \quad (2)$$

H_A^0 being the internal hamiltonian of A. W_A describes the excitation of A by the mean field U_B of nucleus B, whose matrix elements depend on time through the relative coordinate $\mathbf{R}(t)$. The sums over the single particle states, denoted by α and α' , run over both particle and hole states.

2.1 Harmonic approximation

Within RPA, the excited states $|\Psi_\nu\rangle$ of each nucleus are described as superpositions of ph and hp configurations with respect to the ground state $|\Psi_0\rangle$

$$|\Psi_\nu\rangle = q_\nu^\dagger |\Psi_0\rangle = \sum_{ph} [X_{ph}^\nu a_p^\dagger a_h - Y_{ph}^\nu a_h^\dagger a_p] |\Psi_0\rangle \quad (3)$$

where the amplitudes X and Y are solutions of the RPA secular equation, with eigenvalues E_ν . The ground state is defined as the vacuum of the q_ν operators

$$q_\nu |\Psi_0\rangle = 0 \quad (4)$$

In order to avoid unnecessarily complicated expressions, we do not introduce explicitly the coupling to total angular momentum and isotopic spin. When

the RPA phonons are mapped onto bosons [13], the internal hamiltonian of the nucleus can be written as

$$H^0 = \sum_{\nu} E_{\nu} Q_{\nu}^{\dagger} Q_{\nu} \quad (5)$$

which shows that the excitation spectrum is harmonic. The boson operators Q_{ν}^{\dagger} and Q_{ν} in the above equation are given by

$$Q_{\nu}^{\dagger} = \sum_{ph} [X_{ph}^{\nu} B_{ph}^{\dagger} - Y_{ph}^{\nu} B_{ph}] \quad (6)$$

with the same X and Y amplitudes as in eq.(3) but in terms of the boson images (B_{ph}^{\dagger} and B_{ph}) of the ph operators

$$a_p^{\dagger} a_h \rightarrow B_{ph}^{\dagger} + \dots \quad (7)$$

In the above equation we have indicated only the first term of the boson mapping. Assuming that the external field induces only small deformations of the density, only ph and hp terms contribute to W_A and one gets

$$W_A(t) = \sum_{ph} \langle p | U_B(\mathbf{R}(t)) | h \rangle a_p^{\dagger} a_h + h.c. \quad (8)$$

By introducing the boson mapping of eq.(7), it can be rewritten as

$$W_A(t) = \sum_{\nu} W_{\nu}^{10}(t) Q_{\nu}^{\dagger} + h.c. \quad (9)$$

with

$$W_{\nu}^{10} = \langle \Psi_{\nu} | W(t) | \Psi_0 \rangle \quad (10)$$

The independent multiphonon picture is based on eqs. (5) and (9). Within this picture, the Schrödinger equation can be solved exactly and the state of each nucleus at time t is found to be the coherent state

$$|\Phi(t)\rangle = \prod_{\nu} e^{-\frac{1}{2}|I_{\nu}(t)|^2} \sum_{n_{\nu}} \frac{[I_{\nu}(t)]^{n_{\nu}}}{n_{\nu}!} e^{-in_{\nu}E_{\nu}t} (Q_{\nu}^{\dagger})^{n_{\nu}} |0\rangle \quad (11)$$

with

$$I_{\nu} = \int_{-\infty}^t W_{\nu}^{10}(t') e^{-in_{\nu}E_{\nu}t'} dt' \quad (12)$$

where the integral is performed along the relative motion trajectory corresponding to a definite impact parameter. The probability amplitude to excite one- or two-phonon states is calculated by projecting eq. (11) on the corresponding states

$$|\nu\rangle = Q_{\nu}^{\dagger} |0\rangle \quad (13)$$

$$|\nu\nu'\rangle = (1 + \delta_{\nu\nu'})^{-1/2} Q_{\nu}^{\dagger} Q_{\nu'}^{\dagger} |0\rangle \quad (14)$$

where $|0\rangle$ is the vacuum of the Q_ν^\dagger operators. Finally, the cross sections are obtained by integrating the relevant probabilities over the impact parameter.

2.2 Non-linear excitation

In this section we present an approach to go beyond the independent multi-phonon picture by eliminating its two main limitations, the first in the external field and the second in the internal hamiltonian. Let us first consider the pp and hh contributions to the sums in eq.(2), which are neglected in the linear approximation for the external field. Assuming the same boson mapping, truncated at the lowest order, it is easily shown [9] that the mappings

$$a_p^\dagger a_{p'} \rightarrow \sum_h B_{ph}^\dagger B_{p'h} \quad (15)$$

$$a_h a_{h'}^\dagger \rightarrow \sum_p B_{ph}^\dagger B_{ph'} \quad (16)$$

are exact, in the sense that they preserve the commutation relations between fermion-pair operators. Using these relations, the inclusion of the pp and hh terms in eq.(2) gives a W quadratic in the boson operators B_{ph}^\dagger and B_{ph} . By expressing the latter in terms of the collective bosons Q_ν^\dagger and Q_ν one gets

$$W = W^{00} + \sum_\nu W_\nu^{10} Q_\nu^\dagger + h.c. + \sum_{\nu\nu'} W_{\nu\nu'}^{11} Q_\nu^\dagger Q_{\nu'} + \sum_{\nu\nu'} W_{\nu\nu'}^{20} Q_\nu^\dagger Q_{\nu'}^\dagger + h.c. \quad (17)$$

where

$$W_\nu^{10} = \sum_{ph} (W_{ph} X_{ph}^{\nu*} + W_{hp} Y_{ph}^{\nu*}) \quad (18)$$

is the standard linear response expression, whereas

$$W_{\nu\nu'}^{11} = \sum_{php'h'} (W_{pp'} \delta_{hh'} - W_{hh'} \delta_{pp'}) (X_{ph}^{\nu*} X_{p'h'}^{\nu'} + Y_{ph}^{\nu*} Y_{p'h'}^{\nu'}) \quad (19)$$

$$W_{\nu\nu'}^{20} = \sum_{php'h'} (W_{pp'} \delta_{hh'} - W_{h'h} \delta_{pp'}) X_{ph}^{\nu*} Y_{p'h'}^{\nu'*} \quad (20)$$

provide new excitation routes.

The matrix elements of U_B depend on the considered excitation mechanism. Since the general discussion we present here is independent of their form, we postpone to the next section the derivation of their expressions in the case of Coulomb excitation at relativistic energy.

The hamiltonian H_A , with the inclusion of the terms W^{11} and W^{20} , is a quadratic form in the Q_ν^\dagger and Q_ν operators. Therefore, a coherent state solution to the Schrödinger equation still exists. We do not exploit this property because it does not hold any more when the anharmonicities are included, as

we are going to do in next subsection. The effects of introducing non-linear terms in the external field can be important, for example, whenever some selection rule disfavors one of the two steps necessary to make the transition from the ground state to a two-phonon state through the action of W^{10} alone. The term $W_{\nu\nu'}^{11}$ describes the transition from the one-phonon state $|\Psi_\nu\rangle$ to $|\Psi_{\nu'}\rangle$ or from a two-phonon state to another one. In ref. [14–16] it was shown that these non-linear terms can lead to an increase of the population of two-phonon states. The term W^{20} induces a direct transition from the ground state to a two-phonon state that can be very important. This effect has been already reported in [8] where the direct matrix element between the ground state and the dipole member of the low-lying $|2^+ \otimes 3^-\rangle$ quintuplet of states in some Sn isotopes was found to be very large. Similar results, but involving double GR states, have been obtained in [17].

2.3 Anharmonic spectrum

Let us now turn our attention to the other limitation of the independent multiphonon picture we have stressed above, namely the assumption that the internal hamiltonian has the harmonic form of eq.(5). The simplest way to go beyond this approximation starts from the observation that in RPA only the *phph* and *pphh* terms of the residual interaction are taken into account. The *pppp* and *hhhh* terms, when expressed by the same boson mapping used before, introduce a coupling between two-phonon states [9] while the remaining, *ppph* and *hhhp*, terms mix one- and two-phonon states. Finally, when considering two-phonon states one should also take care of the possible violation of the Pauli principle. In the boson mapping method the exclusion principle is introduced through high order terms in the boson expansion [9] built to conserve the fermion-pair commutation algebra. In such a way an additional residual interaction between two-phonon states coming from the particle-hole matrix elements is generated [10]. As a result of these different couplings, the eigenstates of the internal hamiltonian of each nucleus are

$$|\Phi_\alpha\rangle = \sum_{\nu} c_{\nu}^{\alpha} |\nu\rangle + \sum_{\nu_1\nu_2} d_{\nu_1\nu_2}^{\alpha} |\nu_1\nu_2\rangle \quad (21)$$

Therefore, the states excited by the external field will be such mixed states and one cannot speak of pure one- or two-phonon excitations any more. However, when a $|\Phi_\alpha\rangle$ state has a strong overlap with a one-phonon state we may discuss the associated cross-section as part of the one-phonon cross-section. Conversely, if the $|\Phi_\alpha\rangle$ state is dominated by its two-phonon components we may speak about two-phonon strength.

For example, let us consider a state $|\Phi_\alpha\rangle$ which strongly overlaps with a two-phonon state, i.e. whose largest component is $|\nu_1\nu_2\rangle$. In addition to the

possible excitation of $|\Phi_\alpha\rangle$ via this two-phonon component, this state can also be excited by W^{10} through its one-phonon components. However, the energy E_α of $|\Phi_\alpha\rangle$ will be not far from $E_{\nu_1} + E_{\nu_2}$. Therefore, it will contribute to the cross section at that energy. In this sense, because of its structure and of its energy, one may say that it contributes to the two-phonon cross section. This fact was disregarded in ref. [18], where the mixing of a huge number of one- and two- phonon states was considered. A good description of the width of the GDR was thus achieved. However, all the $|\Phi_\alpha\rangle$ states were considered to be one-phonon states when they were excited through their one-phonon components while the two-phonon excitations were calculated in [18] as the transition to states of the form $|\Phi_\alpha \otimes \Phi_{\alpha'}\rangle$. Therefore, that calculation is somewhat equivalent to consider a harmonic spectrum with the states $|\Phi_\alpha\rangle$ as the elementary quanta.

2.4 Time-dependent excitation process

The cross section is calculated, non perturbatively, by solving the Schrödinger equation in the space of the ground state and the $|\Phi_\alpha\rangle$ states. Then the time dependent state, $|\Psi(t)\rangle$, of the nucleus can be expressed as

$$|\Psi(t)\rangle = \sum_{\alpha} A_{\alpha}(t) e^{-iE_{\alpha}t} |\Phi_{\alpha}\rangle \quad (22)$$

where the ground state is also included in the sum as the term $\alpha = 0$. The amplitudes $A_{\alpha}(t)$ are solutions of the set of linear differential equations

$$\dot{A}_{\alpha}(t) = -i \sum_{\alpha\alpha'} e^{i(E_{\alpha}-E_{\alpha'})t} \langle \Phi_{\alpha} | W(t) | \Phi_{\alpha'} \rangle \quad (23)$$

and the probability of exciting the internal state $|\Phi_{\alpha}\rangle$ is given by

$$P_{\alpha} = |A_{\alpha}(t = +\infty)|^2 \quad (24)$$

for each impact parameter. Finally, by integrating P_{α} over the impact parameter we obtain the cross section

$$\sigma_{\alpha} = 2\pi \int_0^{+\infty} P_{\alpha}(b) T(b) b db, \quad (25)$$

where the transmission coefficient $T(b)$ has been taken equal to a sharp cut-off function $\theta(b - b_{min})$. The parameter b_{min} is usually chosen such that the contribution from the nuclear part can be neglected.

3 Relativistic Coulomb excitation

Let us now look in detail the multipole expansion of the external field of eq.(2). Alder and Winther [19] have worked out an analytic expression for the Fourier transform of the semiclassical electromagnetic field in relativistic nucleus-nucleus collisions, with the assumptions that the projectile follows a straight-line trajectory and that the charge densities of both nuclei do not overlap. Therefore, to get the time dependence of the electromagnetic coupling potential the inverse Fourier transform of the expressions derived in [19] can be taken. This procedure has the advantage that the multipole expansion of the time dependent coupling potential is readily known as well as its electric and magnetic components.

Let us introduce the Fourier components of the time dependent coupling potential

$$W(t) = \frac{1}{2\pi} \int_{-\infty}^{+\infty} e^{-i\omega t} W(\omega) d\omega \quad (26)$$

Introducing the expansion of the external field in multipoles $W^{\lambda\mu}$

$$W(t) = \frac{1}{2\pi} \sum_{\lambda,\mu} \int_0^{+\infty} (e^{i\omega t} (-1)^{\lambda+\mu} + e^{-i\omega t}) W^{\lambda\mu}(\omega) d\omega \quad (27)$$

where we have taken into account the behaviour of the multipoles $W^{\lambda\mu}$ for negative ω .

It is shown in ref. [19] that the contribution to $W(\omega)$ of the (λ, μ) multipole can be expressed in terms of electric ($\pi = E$) and magnetic ($\pi = M$) one-body operators

$$W^{\lambda\mu}(|\omega|) = \frac{Z_p e}{v\gamma} \sum_{\pi} G_{\pi\lambda\mu} \left(\frac{c}{v}\right) (-1)^{\mu} K_{\mu}(\beta\omega) \sqrt{2\lambda+1} \left(\frac{\omega}{c}\right)^{\lambda} \mathcal{M}_{\pi}(\pi\omega\lambda - \mu) \quad (28)$$

where $\beta\omega$ is the adiabaticity parameter related to the impact parameter b and to the Lorentz contraction factor, γ , and where K_{μ} are the modified Bessel functions. The expressions of the functions $G_{\pi\lambda\mu}$ can be found in ref. [19].

The 2^{λ} -pole electric transition operator is given by

$$\mathcal{M}(E\omega\lambda\mu) = \frac{(2\lambda+1)!! c^{\lambda}}{\omega^{\lambda+1}(\lambda+1)} \int \mathbf{J}(\mathbf{r}) \cdot \nabla \wedge \mathbf{L} \left(j_{\lambda} \left(\frac{\omega r}{c} \right) Y_{\lambda\mu}(\hat{r}) \right) d^3 r \quad (29)$$

where \mathbf{J} is the current density operator while j_{λ} is a spherical Bessel function.

This operator can also be written down [13] as

$$\begin{aligned} \mathcal{M} (E\omega\lambda\mu) &= \frac{(2\lambda + 1)!!c^\lambda}{\omega^\lambda(\lambda + 1)} \\ &\times \int \left\{ \rho(\mathbf{r})Y_{\lambda\mu}(\hat{r})\frac{\partial}{\partial r}(rj_\lambda(\frac{\omega r}{c})) + i\frac{\omega}{c^2}\mathbf{J}(\mathbf{r}) \cdot \mathbf{r}Y_{\lambda\mu}(\hat{r})j_\lambda(\frac{\omega r}{c}) \right\} d^3r \end{aligned} \quad (30)$$

where the charge density operator $\rho(\mathbf{r})$ has been introduced. The second term will be neglected since, relative to the first, it is of the order of $\hbar\omega/2m_p c^2$.

To get the time dependent coupling potential as the Fourier transform (27-28), we need the transition operators at any value of ω . Since the argument of the spherical Bessel function in the operator is $\omega r/c$, the dependence on ω and r of the multipole $W^{\lambda\mu}$ will not factorize. Therefore there would be no factorization of the time and r dependence in the coupling potential. However, in the limit of long wavelengths, the first term in expression (30) reduces to the well-known static electric multipole operator,

$$\mathcal{M}(E\omega\lambda\mu) \simeq \hat{Q}_{\lambda\mu} = \int \rho(\mathbf{r})r^\lambda Y_{\lambda\mu}(\hat{r})d\mathbf{r} \quad (31)$$

which does not depend on ω . In a similar way, the general magnetic operator

$$\mathcal{M}(M\omega\lambda\mu) = -i\frac{(2\lambda + 1)!!c^{\lambda-1}}{\omega^\lambda(\lambda + 1)} \int \mathbf{J}(\mathbf{r}) \cdot \mathbf{L}(j_\lambda(\frac{\omega r}{c})Y_{\lambda\mu}(\hat{r}))d\mathbf{r} \quad (32)$$

in the limit of long wavelengths, becomes

$$\mathcal{M}(M\omega\lambda\mu) \simeq \hat{M}_{\lambda\mu} = \frac{1}{c(\lambda + 1)} \int (\mathbf{r} \wedge \mathbf{J}(\mathbf{r})) \cdot (\nabla r^\lambda Y_{\lambda\mu}(\hat{r}))d\mathbf{r} \quad (33)$$

That means that, in the limit of long wavelengths, neither the electric nor the magnetic transition operators depend on ω (we will therefore omit ω in the arguments of \mathcal{M}) and they will come out of the integral in (27). We just need to know

$$H_{\lambda\mu}(\beta, t) = \int_0^{+\infty} (e^{i\omega t}(-1)^{\lambda+\mu} + e^{-i\omega t})\omega^\lambda K_\mu(\beta\omega)d\omega \quad (34)$$

with $\mu \geq 0$. $H_{\lambda\mu}(\beta, t)$ is an analytic function whose explicit expression can be found in the appendix.

Therefore, in the long wavelength limit, the following analytic expression of the time dependent coupling potential

$$\begin{aligned} W(t) &= \frac{Z_p e}{2\pi v \gamma} \sum_{\pi\lambda\mu} G_{\pi\lambda\mu}(\frac{c}{v})(-1)^\mu \frac{\sqrt{2\lambda+1}}{c^\lambda} H_{\lambda\mu}(\beta, t) \mathcal{M}(\pi\lambda - \mu) \\ &= \sum_{\pi\lambda\mu} g_{\pi\lambda\mu}(\beta, t)(-1)^\mu \mathcal{M}(\pi\lambda - \mu)/e \end{aligned} \quad (35)$$

can be explicitly derived. From the use of the static multipole operators has followed that any of the term in the sum factorize into two elements, the first one depending on collisions properties, the second one acting on the nucleus being excited.

If one considers only the electric components, which are the most important, only natural parity states can be excited in a first order calculation. However, in a coupled channel calculation, as the present one, non natural parity states have to be included since they can be reached, for example, through a two step process. However we will see in the following that these contributions remain small.

We want to have a feeling about the limits that the use of the static electric operator imposes on the interpretation of our results. If a first-order harmonic and linear calculation was to be done, we could just compare the complete matrix elements $\langle I_f || \mathcal{M}(E\omega_{if}\lambda) || I_i \rangle$ and the approximate one $\langle I_f || \hat{Q}_\lambda || I_i \rangle$. The matrix elements connecting the ground state with one phonon states are consistent within a maximum of a few per thousand for low-lying states, and differ by a few percent when the GDR or the ISGQR are considered.

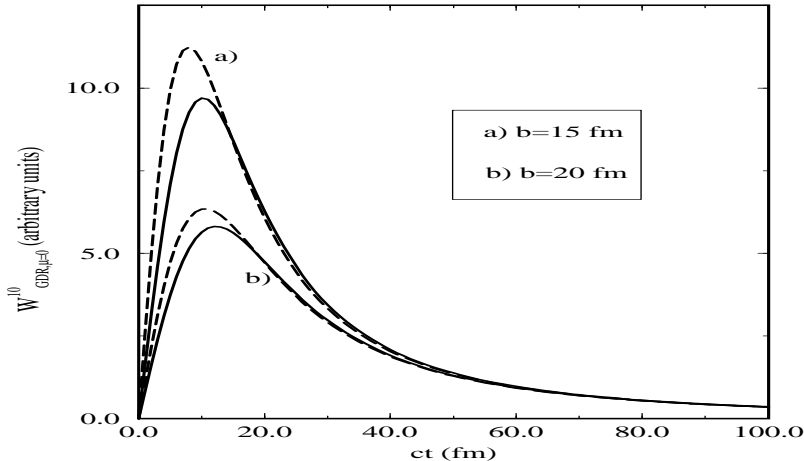


Fig. 1. Matrix element of the coupling potential between the ground state of ^{208}Pb and its GDR with magnetic quantum number zero, as function of time. There are two groups of lines corresponding to two different impact parameters. The solid lines have been obtained using the general expression (see eq. 30) of the electric dipole operator, while to get the dashed line the static expression (eq. 31) has been used.

In a coupled-channel calculation not just a fixed ω_{if} , but the full range of ω

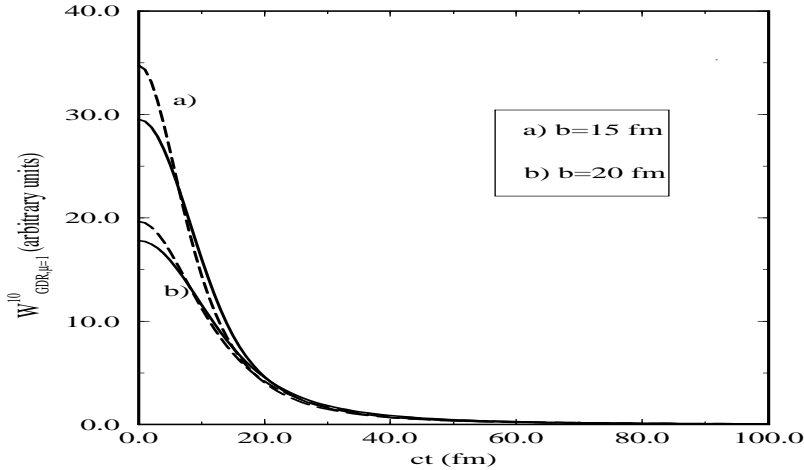


Fig. 2. As figure 1, but for magnetic quantum number one.

values will contribute to the Fourier transform (26- 28). As an illustration, let us consider the colliding system $^{208}\text{Pb}+^{208}\text{Pb}$ at $E_{lab}= 641$ MeV to compare the exact multipole expansion with the long wavelength limit. The associated time-dependent transition matrices from the ground state to the giant dipole resonance, $\langle GDR, \mu|W(t)|0 \rangle$, are presented in figure 1 for the magnetic quantum number $\mu = 0$ and in figure 2 for $\mu = 1$ for two different values of the impact parameter. The solid lines correspond to calculations in which the general expression of the electric multipole operator has been taken into account, and the inverse Fourier transform of the corresponding amplitude has been carried on numerically. The dashed lines correspond to the use of the static electric operator and the analytic expression (35). We can see that qualitatively the time dependence is well reproduced, while the quantitative agreement gets better as the impact parameters increases. That is essentially due to the adiabatic cutoff that the modified Bessel function $K_{\mu}(\beta\omega)$ introduces. This function decays exponentially when the argument becomes bigger than 2 [20]. Therefore, if the impact parameter increases the relevant range of ω in the integral is reduced and we get closer to the long wavelength limit expression for the interacting potential. This effect can be seen in figure 3 where the behaviour with the impact parameter of $\langle GDR, \mu = 1|W(t = 0)|0 \rangle$ is presented at $t=0$. This is the time at which the difference between both approaches is maximum when $\lambda + \mu$ is even. A similar behaviour is found when the matrix elements W^{11} or W^{20} are considered.

The conclusion of this study is that, in the excitation energy region we will consider, it is reasonable to use the static electric operator. This amounts to a

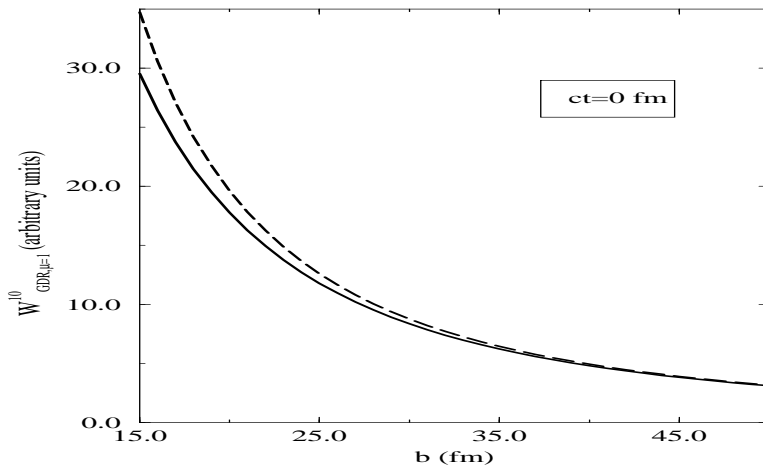


Fig. 3. Impact parameter dependence of the matrix element of the coupling potential at time $t=0$ between the ground state of ^{208}Pb and its GDR with magnetic quantum number one.

considerable saving of calculations since, for each multipole, the time and the r dependence factorize.

4 Results about the excitation of ^{208}Pb

Let us now apply the above formalism to a specific nucleus, namely the ^{208}Pb excited in a collision with a Pb nucleus at 641 MeV per nucleon. We will first discuss the effect of the anharmonicities on the RPA spectrum. Secondly, we will look at the effect of non-linear terms in the external field. Finally, we will consider the influence of both these terms on the excitation probability and the cross sections.

4.1 Energy spectrum

The one-phonon basis is calculated in the self-consistent RPA with SGII Skyrme interaction [21]. Although we are using an explicit neutron proton representation the isospin results to be a rather good quantum number as far as collective states are concerned. We have selected all the states which exhaust at least 5% of the appropriate EWSR and, for a particular spin and parity

Table 1

One-phonon basis for the nucleus ^{208}Pb . For each state its spin and parity, isospin, energy and percentage of the EWSR are reported.

Phonons	J^π	T	$E(\text{MeV})$	$\%EWSR$
GMR_1	0^+	0	13.610	61
GMR_2	0^+	0	15.022	28
GDR_1	1^-	1	12.435	63
GDR_2	1^-	1	16.662	17
2^+	2^+	0	5.545	15
$ISGQR$	2^+	0	11.599	76
$IVGQR$	2^+	1	21.815	45
3^-	3^-	0	3.464	21
$HEOR$	3^-	0	21.302	37

(and isospin), we have grouped together the ones which are closer in energy according to the method described in ref. [9]. We have considered the one-phonon states reported in table 1, i.e. the various components of the isoscalar monopole resonance (GMR), the components of the isovector dipole resonance (GDR), the low-lying 2^+ state and the quadrupole resonances, both isoscalar ($ISGQR$) and isovector ($IVGQR$), and finally the collective low-lying (3^-) and high-lying ($HEOR$) isoscalar octupole states.

We have then constructed the residual interaction between the one- and two-phonon states and also among the two-phonon states. The two-phonon states are coupled to a total angular momentum and parity. In the case of the 1^- states, while the coupling between one- and two-phonon states is of the order of 1/2 MeV up to 1 MeV, the coupling between two-phonon states is, in average, about one order of magnitude smaller.

Then for each spin and parity the total matrix has been diagonalised in order to get the states $|\Phi_\alpha\rangle$. Since these states are always dominated by one component we have decided to label them by the name of this dominant component. Table 2 gives for all 1^- states the total shift ΔE (in KeV) from the unperturbed energy E_0 and their component on the GDR. Tables 3 and 4 contain some information on the results of the diagonalization for the low lying and the high lying two-phonon states, respectively (see caption). We have re-

Table 2

Characteristics of the $|\phi_\alpha\rangle$ dipole 1^- states resulting from the diagonalization of the internal hamiltonian. In the first column we indicate the dominant component. The values in the second column remind us the energies associated with this component in the harmonic approach. The shift in the energy produced by the anharmonicities is indicated by ΔE (in KeV). We can compare these values with the diagonal matrix elements of the residual interaction, ΔE_0 (in KeV). In the last columns we report the amplitude with which the GDR's appear in such mixed states.

Dipole	States	$E_0(\text{MeV})$	ΔE	(ΔE_0)	c_{GDR_1}	c_{GDR_2}
GDR_1		12.435	-132.	(0.)	0.993	-0.006
GDR_2		16.662	-56.	(0.)	0.002	0.994
$3^- \otimes 2^+$		9.009	195.	(200.)	0.023	0.000
$3^- \otimes ISGQR$		15.062	75.	(67.)	0.045	0.000
$GDR_1 \otimes 2^+$		17.981	-207.	(-220.)	0.043	0.082
$GDR_2 \otimes 2^+$		22.207	-23.	(-36.)	0.007	0.048
$GDR_1 \otimes ISGQR$		24.034	33.	(-10.)	0.057	-0.004
$3^- \otimes IVGQR$		25.278	6.	(4.)	-0.014	0.000
$GDR_1 \otimes GMR_1$		26.046	18.	(-27.)	0.057	0.000
$HEOR \otimes 2^+$		26.847	25.	(24.)	-0.004	0.000
$GDR_1 \otimes GMR_2$		27.458	-10.	(-35.)	0.039	0.000
$GDR_2 \otimes ISGQR$		28.261	-88.	(-51.)	0.007	0.054
$HEOR \otimes ISGQR$		32.901	-31.	(-30.)	-0.004	0.000
$GDR_1 \otimes IVGQR$		34.250	-44.	(-47.)	-0.007	0.000
$GDR_2 \otimes IVGQR$		38.477	-174.	(-174.)	0.006	0.000
$HEOR \otimes IVGQR$		43.117	-49.	(-53.)	-0.011	0.000

stricted these tables to natural parity states since the non natural parity states are essentially not mixed and weakly excited. Moreover, states with angular momentum greater than 3 have not been included since they do not play an important role in Coulomb excitation processes. From these tables one can see that the anharmonicities predicted by our microscopic calculations are small, the typical shifts in energy (ΔE) being a few hundred keV. Each multiplet appears to be splitted with a characteristic spreading equal to the global shift.

Table 3

As table 2, but for the low lying states with natural parity. In the first column we give the dominant component while in the last one we report the second most important component and its coefficient.

States	$E_0(\text{MeV})$	J^π	ΔE	(ΔE_0)	c_{conf}	Config.
3^-	3.464	3^-	-256.	(0.)	0.093	$3^- \otimes 2^+$
2^+	5.545	2^+	-364.	(0.)	-0.201	$3^- \otimes 3^-$
$3^- \otimes 3^-$	6.927	0^+	958.	(1137.)	-0.163	GMR_1
		2^+	381.	(400.)	0.195	2^+
$3^- \otimes 2^+$	9.009	1^-	195.	(200.)	-0.024	GDR_1
		3^-	161.	(112.)	-0.091	3^-
$2^+ \otimes 2^+$	11.090	0^+	136.	(145.)	-0.055	$3^- \otimes 3^-$
		2^+	178.	(30.)	-0.158	2^+
$GDR_1 \otimes 2^+$	17.981	1^-	-207.	(-220.)	-0.083	GDR_2
		3^-	-4.	(-4.)	-0.010	$GMR_1 \otimes 3^-$

The mixing coefficients are in average also small, around 0.05 and at maximum around 0.2.

4.2 Excitation Processes

Let us now study the characteristics of the excitation strength. We have seen that the excitation operator contains 3 parts. The first one is the linear response which is usually taken into account in the standard calculations: i.e. in the harmonic and linear picture. The strength associated to the operator W^{10} is, in this picture, concentrated in the one-phonon states. The introduction of a mixing between states with different numbers of phonons spreads the strength over more states. For instance, in the case of the GDR the strength will be distributed among the dipole states of tables 2 in a fashion proportional to the c 's coefficients. Analogously, the strength W^{20} initially located around

Table 4

Same as table 3, but for mixed states with natural parity and with energies between 22 and 29 MeV.

States	$E_0(\text{MeV})$	J^π	ΔE	(ΔE_0)	c_{conf}	Config.
$GDR_2 \otimes 2^+$	22.207	1^-	-23.	(-36.)	-0.046	GDR_2
		3^-	-66.	(-64.)	-0.018	$GDR_2 \otimes ISGQR$
$ISGQR \otimes ISGQR$	23.198	0^+	4.	(3.)	0.014	$GDR_1 \otimes GDR_1$
		2^+	35.	(-15.)	-0.061	$ISGQR$
$GDR_1 \otimes ISGQR$	24.034	1^-	33.	(-10.)	-0.057	GDR_1
		3^-	-2.	(-2.)	0.010	$3^- \otimes IVGQR$
$3^- \otimes HEOR$	24.766	0^+	34.	(14.)	0.133	$GDR_1 \otimes GDR_1$
		2^+	22.	(-2.)	0.225	$GDR_1 \otimes GDR_1$
$GDR_1 \otimes GDR_1$	24.871	0^+	41.	(33.)	-0.132	$3^- \otimes HEOR$
		2^+	-189.	(-192.)	-0.223	$3^- \otimes HEOR$
$GMR_1 \otimes ISGQR$	25.210	2^+	42.	(11.)	-0.048	$ISGQR$
$IVGQR \otimes 3^-$	25.278	1^-	6.	(4.)	0.015	GDR_1
		3^-	-24.	(-25.)	-0.018	$HEOR$
$GMR_1 \otimes GDR_1$	26.046	1^-	18.	(-27.)	-0.057	GDR_1
$GMR_2 \otimes ISGQR$	26.621	2^+	25.	(8.)	-0.033	$ISGQR$
$2^+ \otimes HEOR$	26.847	1^-	25.	(24.)	0.007	$GMR_2 \otimes GDR_1$
		3^-	-39.	(-44.)	-0.018	$HEOR$
$GMR_1 \otimes GMR_1$	27.221	0^+	297.	(56.)	-0.128	GMR_1
$2^+ \otimes IVGQR$	27.360	0^+	-196.	(-195.)	-0.016	$ISGQR \otimes IVGQR$
		2^+	-84.	(-90.)	-0.032	$IVGQR$
$GMR_2 \otimes GDR_1$	27.458	1^-	-10.	(-35.)	-0.042	GDR_1
$GDR_2 \otimes ISGQR$	28.261	1^-	88.	(51.)	-0.055	GDR_2
		317	-60.	(-62.)	0.010	$2^+ \otimes GDR_2$
$GMR_1 \otimes GMR_2$	28.633	0^+	254.	(74.)	-0.100	$GMR_2 \otimes GMR_2$

the two-phonon states, after the diagonalisation will be distributed over many states.

Moreover, the various states have now two paths to be excited in one step, either through the W^{10} excitation of their one-phonon component or via the W^{20} interaction exciting directly their two-phonon part. Now, depending on the respective sign of the mixing coefficients, these two contributions may interfere constructively or destructively.

In addition to these direct transitions from the ground-state, the term W^{11} of the external field may induce transitions between excited states. These new excitation routes may modify the distribution of the excitation probabilities associated with different states. In the next subsection we will give a few examples where we will show the importance of the W^{11} and W^{20} terms and of the anharmonicities.

4.3 Excitation cross-sections

Let us now put all these ingredients together in order to compute the excitation probabilities and cross sections. All the natural parity states with angular momentum less or equal to 3 have been included in the calculations while for the non natural parity states we have included only the 1^+ and the 2^- ones. By solving the coupled equations (23) we get the probability amplitude for each $|\phi_\alpha\rangle$ state, from which we calculate the cross section by integrating over the various impact parameters associated with Coulomb inelastic excitations. The b_{min} has been chosen according to the systematics of ref [22]. We will describe in detail the results for the $^{208}\text{Pb}+^{208}\text{Pb}$ system at 641 MeV/A and we will first focus our discussion on the excitation of dipole states.

In fig. 4 we present the dipole excitation cross-section as predicted using various approximations in order to disentangle the effects of the anharmonicities and non-linearities coming from W^{11} and W^{20} . We have run several calculations corresponding to the various cases we can have, by switching on and off the different terms of the external field. From the figure it is clear that the spectrum is dominated by the dipole resonance. However, one can observe important modifications of the dipole strength for the different calculations compared with the harmonic and linear prediction.

In particular, states which were not excited in the harmonic and linear picture can reach a sizeable cross-section when all the different corrections are taken into account. For instance, this is the case for the state around 9 MeV, which is mostly built out of the 1^- component of the states resulting from the coupling of the low-lying 3^- and 2^+ . In the first line of table 5, the Coulomb inelastic cross-sections for this state at several degrees of approximation are given. One

$$^{208}\text{Pb} + ^{208}\text{Pb}, E_{\text{lab}} = 641 \text{ MeV/A}, L = 1$$

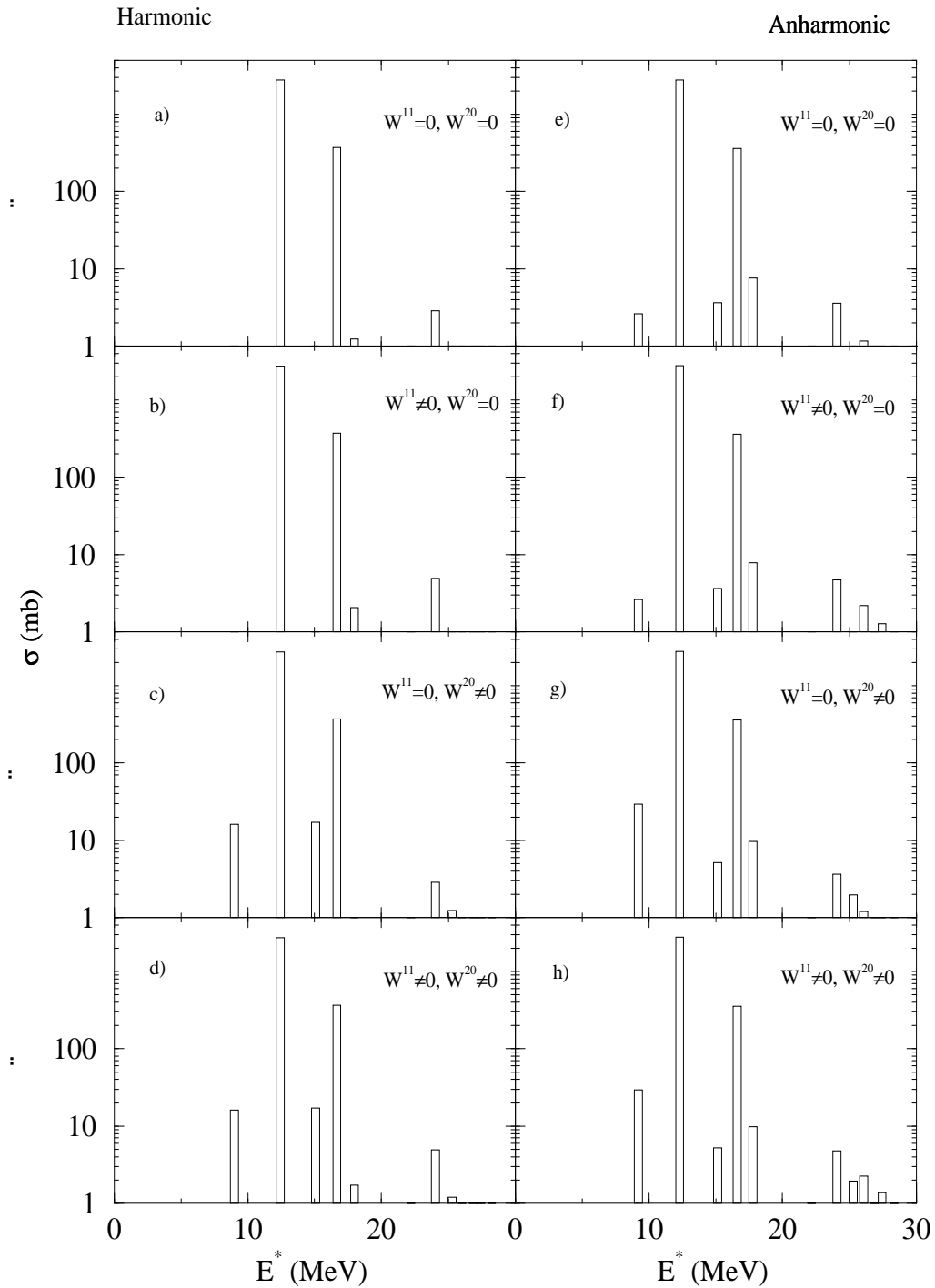


Fig. 4. Relativistic Coulomb target dipole excitation cross section for the $^{208}\text{Pb}+^{208}\text{Pb}$ system at 641 MeV/A. Each bar corresponds to the cross section of a single state.

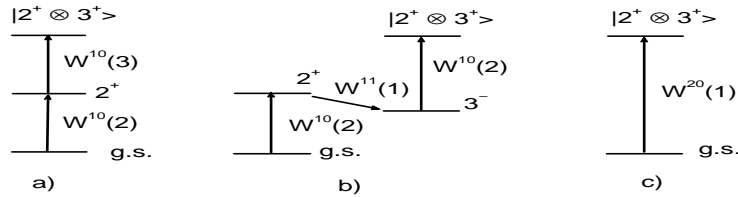


Fig. 5. Schematic representation of the Coulomb excitation of the $|2^+ \otimes 3^- \rangle$ state.

can see that this two-phonon state is almost not excited in the harmonic and linear picture. Indeed, at this level of approximation, the most direct way to excite this state requires one E3 and one E2 transitions (see figure 5.a) which are not favourable. In this case the W^{11} term does not help much because either we reach the state by one E1 plus two E2 transitions, as in figure 5.b, or by one E3 plus two E1 if in the first step we excite the 3^- state. In any case, at least one of the involved transitions is of high multipolarity. Conversely, the direct transitions due to the W^{20} terms (see fig. 5.c) increases the cross section by a huge factor, bigger than 500. Indeed, this term is now a dipole transition which is strongly favoured. The importance of W^{20} will decrease as the excitation energy of the state increases. For instance, the enhancement factor 500 reduces to about 50 for the dipole states $|2^+ \otimes HEOR \rangle$ or $|ISGQR \otimes HEOR \rangle$ whose energies are around 30 MeV.

When the mixing of one- and two-phonons states is taken into account this state can be also populated by W^{10} through its small GDR component (see table 2). In fact, although the c coefficient of the GDR component is small, this component gives a considerable contribution due to the fact that it is a one step dipole excitation. Moreover, the energy of the state (about 9 MeV) is lower than the one of the GDR state. All together the effect of the anharmonicities on the inelastic cross section is a factor about 100 times bigger with respect to our reference calculation.

Finally, when all these different contributions are taken into account this dipole two-phonon state built from low-lying 3^- and 2^+ is receiving 30 mb cross

Table 5

Coulomb inelastic target excitation cross sections (in mb) for the $^{208}\text{Pb}+^{208}\text{Pb}$ system at 641 MeV/A and for the mixed states which are identified by their dominant component (first column) and their angular momenta and parity (second column). In the third column is shown the reference result corresponding to a harmonic and linear calculation. In the fourth column the additional inclusion of only the W^{11} non-linear term is allowed. Similarly, in the fifth column the only difference with the reference calculation is due to the addition of only the W^{20} non-linear term. In the sixth column the results of an anharmonic and linear calculation are presented. The last column correspond to results of the anharmonic and non-linear approach.

States	J^π	harm. & lin.	W^{11}	W^{20}	anharm.	anharm. & non-lin.
$2^+ \otimes 3^-$	1^-	0.03	0.04	16.21	2.60	29.53
$ISGQR \otimes 3^-$	1^-	0.05	0.07	17.22	3.63	5.18
$22 < E < 28$ (MeV)	1^-	3.55	5.95	5.07	6.42	12.18
$2^+ \otimes GDR_1$	1^-	1.24	2.07	0.99	7.64	9.83
$ISGQR$	2^+	298.91	332.56	300.09	278.35	314.18

section, while in the harmonic and linear limit it was just 0.03 mb.

In this case the effects of non-linearities and anharmonicities interfere constructively. That is not a general property. An example in which these effects interfere destructively is shown in table 5, where the excitation cross section to the dipole state $|ISGQR \otimes 3^- \rangle$ is given. In order to clarify this mechanism we have done a parametric calculation in which only three single phonon states were considered, namely the 3^- , the 2^+ and the GDR. Then we have mixed the single phonon $|GDR \rangle$ with the two phonon state $|2^+ \otimes 3^- \rangle$, coupled to a total spin 1, in the following way

$$\begin{aligned}
|\Phi_1 \rangle &= \cos \beta |2^+ \otimes 3^- \rangle + \sin \beta |GDR \rangle \\
|\Phi_2 \rangle &= -\sin \beta |2^+ \otimes 3^- \rangle + \cos \beta |GDR \rangle
\end{aligned} \tag{36}$$

Increasing the parameter $|\beta|$ we can go from a pure harmonic case ($\beta = 0$) to a very strong anharmonicity. Changing the β sign the relative phases of

Table 6

Same as table 5, but for the parametric state $|\Phi_1\rangle$ of eq. (36). In the last column the values of the parameter β used.

harm. & lin.	W^{11}	W^{20}	anharm.	anharm. & non-lin.	$\sin \beta$
0.26	0.27	16.58	1.96	29.71	-0.02
			1.92	7.20	0.02

the $|\Phi_\alpha\rangle$ components are changed. The energies of the states were kept fixed and equal to the energy, in the harmonic limit, of the main component; i.e. $E_1 = E_{2^+} + E_{3^-}$ and $E_2 = E_{GDR}$.

The cross sections corresponding to the $|\Phi_1\rangle$ state are shown in table 6 for two opposite values of β . From the table, we can see that the behaviour of the cross section is very similar to the one obtained in the complete calculation (see table 5). Indeed the results for $\beta = -0.02$ are similar to the ones obtained for the $|2^+ \otimes 3^- \rangle$ dipole state, where anharmonicities reinforce the effects of non-linearities on the cross section. Conversely, for $\beta = 0.02$ the final result is much lower than the one given by the W^{20} term alone. This result is very similar to the one obtained for the $|ISGQR \otimes 3^- \rangle$ state shown in table 5.

The reason for this different behaviour can be easily understood in a first order calculation if we take into account the following relations

$$\begin{aligned}
 \langle \nu \lambda \mu | W(t) | 0 \rangle &= g_{E\lambda\mu}(\beta, t) \langle \nu \lambda | V^{10}(E\lambda) | 0 \rangle \\
 \langle [\nu_1 \nu_2] \lambda \mu | W(t) | 0 \rangle &= \frac{1}{\sqrt{1 + \delta_{\nu_1, \nu_2}}} g_{E\lambda\mu}(\beta, t) \langle \nu_1 \lambda_1 \nu_2 \lambda_2 | V^{20}(E\lambda) | 0 \rangle
 \end{aligned} \tag{37}$$

where $g_{E\lambda\mu}$ was defined in equation (35). Let us call σ_1 the cross section corresponding to the state $|\Phi_1\rangle$. In a first order calculation we get

$$\frac{\sigma_1^{\text{anharm\&non-lin}}}{\sigma_1^{\text{harm\&non-lin}}} = \left(\cos \beta + \frac{\sin \beta}{x} \right)^2 \tag{38}$$

where x is given by the following ratio of matrix elements

$$x = \frac{\langle 2^+ \otimes 3^- | V^{20}(E1) | 0 \rangle}{\langle GDR | V^{10}(E1) | 0 \rangle} \tag{39}$$

Since $|x|$ is usually smaller than 1 the second term in equation (38) can be

important even for small anharmonicities. The values of β and x as well as their signs are important.

In the same way we can calculate the cross section σ_2 corresponding to the state $|\Phi_2\rangle$ and get

$$\frac{\sigma_2^{\text{anharm\&non-lin}}}{\sigma_2^{\text{harm\&non-lin}}} = (\cos \beta - x \sin \beta)^2 \quad (40)$$

Since $|x|$ is usually small, the previous ratio will not differ very much from one. Note also that, in first order, $\sigma_2^{\text{harm\&non-lin}}$ and $\sigma_2^{\text{harm\&lin}}$ coincide, while $\sigma_1^{\text{harm\&non-lin}}$ differs from $\sigma_1^{\text{harm\&lin}} = 0$.

Now, it happens that the x ratio for the $|2^+ \otimes 3^- \rangle$ and $|ISGQR \otimes 3^- \rangle$ dipole states has the same sign and similar values: -0.058 and -0.091 , respectively. But the coefficients of their GDR component have opposite sign (see table 2) and their values are such that the dependence of the ratio in equation (38) on β is nearly linear. Then in one case anharmonicities and non-linearities interfere constructively and in the other case interfere destructively. By increasing $|\beta|$ this property is lost and we could have a reinforce effect in σ_1 even if β and x have opposite sign. That is confirmed by the parametric calculation to all orders, as can be seen in figure 6, where we have increased the $|\beta|$ parameter up to about 0.2. That would support that for nuclei with stronger anharmonicities we should get a higher increase in the cross section with respect to the linear and harmonic case.

Of course in this example we have assumed that the mixing has just two components what is a great simplification, specially for the state whose main component is the GDR. Let us go back to the complete calculations where we have a mixing of all the states and their proper energies are taken into account.

Similar effects can also be seen on other states in the dipole response of the Pb nucleus (see table 4). The two-phonon states located around 25 MeV excitation energy are of particular interest. These states are mainly built by coupling the giant dipole with the monopole and quadrupole states. As in the previous case, the direct transition W^{20} and the mixing are important. In addition to that, also the transition between one-phonon states contributes to increase the cross section. Table 5 shows that in such a case the increase of the cross section of these two-phonon states is more than 300%. This reminds the findings discussed in ref [12], where in a very schematic model we were showing that non-linearities and anharmonicities might strongly modify the excitation cross-section. An example where the anharmonicities play an important role is given by the excitation of the $|GDR_1 \otimes 2^+ \rangle$ state whose cross section is reported in table 5. The big increase of the anharmonic and non-linear cross section can

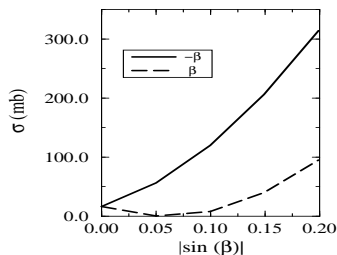


Fig. 6. Relativistic Coulomb target excitation cross section for the parametric calculation of eq. (36) as function of absolute value of the mixing coefficient $\sin \beta$.

be entirely ascribed to its big GDR_2 component (see table 3).

This increase of the cross section is seen not only in the dipole channel, which gets large contributions from the GDR itself, but also for other multipolarities. Let us for instance consider the isoscalar giant quadrupole resonance (ISGQR) (see table 5). Looking at its excitation we see that the inclusion of W^{11} raises the value of σ from 299 mb to 333 mb (in the harmonic case). In this case, besides the direct transition to the GQR due to the action of W^{10} , we are considering the second order one which proceeds first through the excitation of the GDR by $W^{10}(1)$ and then to GQR by means of W^{11} (see fig. 7). This second order process is able to give almost a 12% increase because the excitation probability of the first transition is very high and because the effect of W^{11} is enhanced by the fact that the energies of GDR and GQR are close each other.

We close this detailed analysis with a comment on the effect of the non natural parity states 1^+ and 2^- we have introduced in the calculations. In our calculation we found that the contribution of the 1^+ states is, in this respect, irrelevant and the one of the 2^- , in the region of the DGDR, amounts to about 1 mb. At lower energy, around 16 MeV, its contribution is 2 mb. Similar conclusions have been recently reached in ref.[11].

So far, we have discussed the influence on some particular states. In order to get a global view on the effects of both non-linearities and anharmonicities we must compute the complete inelastic cross section. Therefore, we have summed

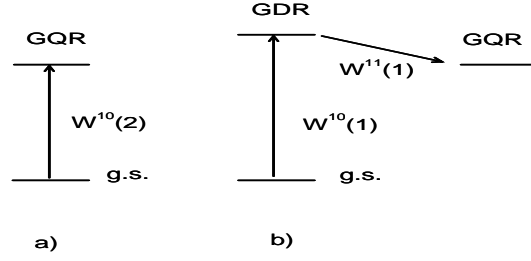


Fig. 7. Schematic representation of the Coulomb excitation of the $|GQR\rangle$ state.

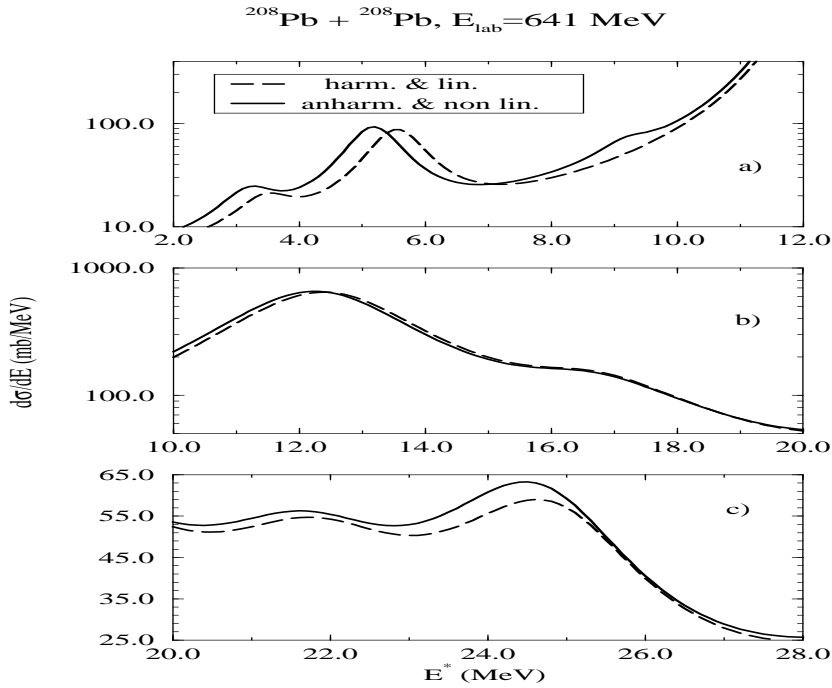


Fig. 8. Relativistic Coulomb target excitation cross section for the $^{208}\text{Pb}+^{208}\text{Pb}$ system at 641 MeV/A as function of the excitation energy. The three parts correspond to different energy regions. The cross section for each $|\Phi_\alpha\rangle$ state has been smoothed by a lorentzian with a 3 MeV width. For the low energy region we used a 1 MeV width.

Table 7

Comparison between our theoretical results and the experimental cross sections (in barn) reported in ref. [6] for the Pb + Pb reaction at 641 MeV per nucleon. The theoretical results (first line) correspond to the sum of all GDR (first column) and all DGDR (second column) cross-section. The third column contains the cross section associated with all the states above the IVGQR ($E > 22$ MeV). The theoretical cross sections are obtained from the non-linear and anharmonic calculation while the numbers in parenthesis refer to the linear and harmonic limit. The experimental results are reported in the second line. The first number corresponds to the extracted GDR cross section while the second number comes from a gaussian fit of the high energy cross section after subtraction of the GDR and GQR single-phonon strength.

	GDR	DGDR	DGDR energy region
σ_{th}	3.13 (3.14)	0.21 (0.22)	0.31 (0.28)
σ_{exp}	3.28 ± 0.05		0.38 ± 0.04

up all the contributions coming from the various states after a smoothing of each individual line shape by a lorentzian. The results are presented in fig. 8. For the low energy region (fig. 8.a) the width of the lorentzian has been chosen equal to 1 MeV, while for the energy region around the GDR (fig. 8.b) and the one around the DGDR (fig. 8.c) it has been fixed equal to 3 MeV. In this figure we can see that the single GDR region is not much affected by the anharmonicities and non-linearities while the cross-section in the DGDR region is increased by 10% when the anharmonicities and non-linearities are taken into account. We would like to point out that this increase is mainly due to the excitation of two-phonon states whose energies are in the DGDR region and whose population has been possible only because of the presence of the anharmonicities and the non-linear terms W^{11} and W^{20} in the external field. The low lying part of the spectrum is also affected and in particular, as we discussed before, a new dipole strength is visible in the 9 MeV region.

In table 7 we show a comparison between our theoretical results and the experimental cross-section for the GDR and the DGDR energy region. The agreement for the GDR seems satisfactory. The theoretical yield associated with the DGDR states explains about 60% of the experimental cross section. However, this disagreement between the experimental cross section in the DGDR region and our theoretical estimate is reduced to $18\% \pm 10\%$ by the inclusion of all the different multiphonon states considered in our calculation and lying above the IVGQR.

In conclusion, both the introduction of different two-phonon states and the

Table 8

Same as table 1, but for ^{40}Ca .

Phonons	J^π	T	$E(\text{MeV})$	% EWSR
GMR_1	0^+	0	18.25	30
GMR_2	0^+	0	22.47	54
GDR_1	1^-	1	17.78	56
GDR_2	1^-	1	22.03	10
$ISGQR$	2^+	0	16.91	85
$IVGQR$	2^+	1	29.53	26
3^-	3^-	0	4.94	14
$LEOR$	3^-	0	9.71	5
$HEOR$	3^-	0	31.33	25

inclusion of anharmonicities and non-linearities are bringing the theoretical prediction rather close to the experimental observation for the Coulomb excitation of Pb nuclei in the DGDR region.

5 Results about the excitation of ^{40}Ca

We have also done calculations for the excitation of ^{40}Ca by a ^{208}Pb projectile with $E_{lab} = 1000\text{MeV}/A$. The one-phonon basis for ^{40}Ca are shown in table 8. We do not have any collective low lying 2^+ state because the RPA does not generate such state for the ^{40}Ca nucleus. The properties of the dipole 1^- states are reported in table 9, which is the analogous of table 2 for ^{208}Pb . We note that we have bigger anharmonicities than in the Pb case.

The coupled channel equations (23) were solved only for the natural parity states which, as we have seen in the case of Pb, are providing the largest contribution to the cross-section. The resulting cross section, after a smoothing by a lorentzian with a 3 MeV width, is shown in fig. 9. The peak at around 18 MeV is due to the GDR_1 with the contribution of the ISGQR state. The shoulder at about 22 MeV is given by the GDR_2 and the two-phonon dipole state $|ISGQR \otimes 3^- \rangle$ which gives, in the anharmonic and non-linear case, a 10% increase. The latter state is excited in the same fashion of the $|ISGQR \otimes$

Table 9
Same as table 2, but for ^{40}Ca .

Dipole	States	$E_0(\text{MeV})$	ΔE	(ΔE_0)	c_{GDR_1}	c_{GDR_2}
GDR_1		17.780	-432.	0.	0.989	-0.006
GDR_2		22.034	-391.	0.	0.004	0.990
$ISGQR \otimes 3^-$		21.851	708.	713.	0.024	0.011
$ISGQR \otimes LEOR$		26.616	231.	224.	0.011	-0.011
$IVGQR \otimes 3^-$		34.541	-125.	-128.	0.001	-0.020
$GDR_1 \otimes ISGQR$		34.690	139.	35.	-0.063	-0.044
$GMR_1 \otimes GDR_1$		36.026	-110.	-214.	-0.075	-0.004
$GDR_2 \otimes ISGQR$		38.943	-21.	-74.	-0.034	0.034
$IVGQR \otimes LEOR$		39.305	-245.	-245.	0.000	0.003
$GMR_1 \otimes GDR_2$		40.280	-175.	-292.	0.011	-0.079
$GMR_2 \otimes GDR_1$		40.249	9.	-202.	-0.098	-0.005
$GMR_2 \otimes GDR_2$		44.502	20.	-194.	0.000	-0.098
$GDR_1 \otimes IVGQR$		47.379	-315.	-308.	-0.011	-0.003
$ISGQR \otimes HEOR$		48.240	-13.	-27.	0.000	0.005
$GDR_2 \otimes IVGQR$		51.633	-270.	-271.	0.001	0.001
$IVGQR \otimes HEOR$		60.929	-271.	-275.	-0.009	0.005

$3^- >$ state of ^{208}Pb , see table 10, with the difference that now the increasing factor is 1000 while in the ^{208}Pb case it was only 100. Finally, we note two interesting energy regions where there is a difference between the harmonic and linear and the anharmonic and non-linear case, namely the regions around 35 and 40 MeV. The sum of the cross section for the 1^- state belonging to these two regions are reported in table 10 for the different kinds of calculations we can make within our approach. From the table we see that the increase is essentially due to the dipole 1^- states and this is an almost pure anharmonic effect. The global increase in the DGDR energy region amounts to a 20%, which is twice what we obtained for Pb.

Table 10
Same as table 5, but for ^{40}Ca .

States	J^π	harm. & lin.	W^{11}	W^{20}	anharm.	anharm. & non-lin.
$ISGQR \otimes 3^-$	1^-	0.004	0.006	6.660	0.284	3.955
$34 < E < 36$ (MeV)	1^-	0.110	0.287	0.295	1.723	2.221
$38 < E < 45$ (MeV)	1^-	0.008	0.020	0.022	1.468	1.698

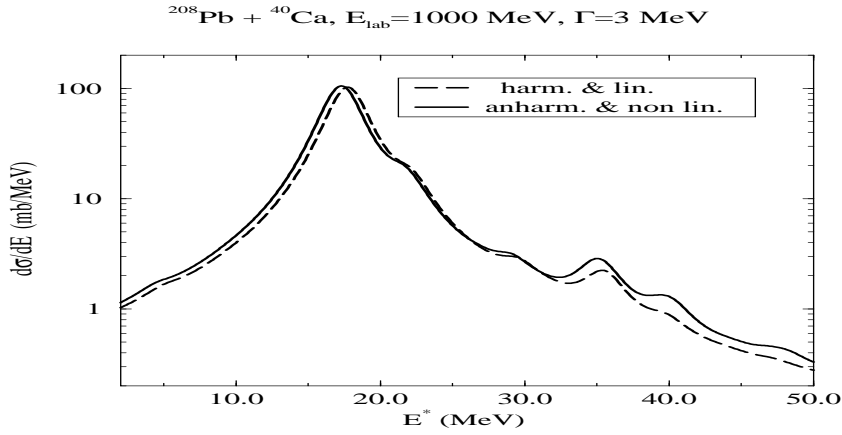


Fig. 9. Relativistic Coulomb target excitation cross section for the $^{208}\text{Pb}+^{40}\text{Ca}$ system at 1000 MeV/A as function of the excitation energy. The cross section for each $|\Phi_\alpha\rangle$ state has been smoothed by a lorentzian with a 3 MeV width.

6 Discussion and conclusion

We have employed an RPA based approach to compute the anharmonicities: We have diagonalized the residual interaction between RPA phonons in the space of one- and two-phonons states. We have taken into account also the

particle-particle and hole-hole terms in the external field making possible the direct excitation of two-phonon states as well as the transition between one-phonon states. These non-linear terms and the anharmonicities are not taken into account in the "standard" approach of the multiphonon picture. Within this framework we have calculated the Coulomb excitation of ^{208}Pb and ^{40}Ca nuclei due to the impinging ^{208}Pb nucleus at 641 and 1000 MeV/A.

In this paper we have shown that the inclusion of both anharmonicities and non-linear terms in the external field reduce the disagreement between the experimental cross section in the DGDR region and the theoretical one calculated within the "standard" approach. Moreover, for the ^{208}Pb case, we have found a big effect also at low energy where the $|2^+ \otimes 3^+ \rangle$ state would have never been excited without the presence of both the anharmonicities and non-linearities. Since these low lying two-phonon states are strongly mixed and since their energy is low, we believe that they could also be strongly excited by the nuclear part of the mean field at an incident energy lower than the one considered here. Theoretical and experimental work in this direction are called for.

In view of our calculations it is clear that non-linearities and anharmonicities have an influence on the Coulomb excitation. On some particular states this influence can be very strong, while averaging over all the states we have found an increase of the cross section by about 10% for Pb and 20% for Ca in the region of the two-phonon states while the energies were modified only by a few percent. However, this might not be the final answer because of different reasons. First, we are working in a truncated subspace in order to keep only one- and two- phonon states. However, we know that a large part of the increase observed in ref. [12] is due to the increase of transition matrix elements coming from components of the wave function containing large phonon numbers. These components are not taken into account in the present calculation and this reduces the influence of anharmonicities. In fact we have tested this point on the simple model reported in reference [12] and we have observed that a truncation of the multiphonon space at the two-phonon level reduces the increase of the cross section by almost a factor 4. Unfortunately, this point is not easy to improve because the computation time will become too long if we are forced to include more multiphonon states. We are now trying to develop an alternative approach based on time-dependent mean field theory in the boson representation.

The anharmonicities we are computing are mainly due to the residual interaction into channels which are different from the usual particle-hole interaction. One may argue that, as far as effective interactions are concerned, their parameters are only fitted close to the ground state. Therefore, except for the particle-hole channel the other parts of the interaction are not really constrained by the theory. However, in some cases the residual interaction has

been tested far from the ground state. In this respect the relative success of the time-dependent mean field theory (and other treatments such as adiabatic TDHF or generator coordinate method) might be an indication that the same Skyrme parametrisation also holds for large amplitude motion. However, this point is certainly calling for more theoretical developments in order to better define the effective interaction in channels different from the standard particle-hole ones.

From the experimental point of view it seems that the ^{208}Pb nucleus behaves as a rather good vibrator. In fact the discrepancy about the cross-section between theory and experiment is apparently much smaller in the case of Pb than in the case of Xe [6]. Moreover, as far as the shift in energy of the two-phonon state with respect to the harmonic limit is concerned, a shift of less than 1% was found experimentally for Pb while for Xe it was of the order of 10% [4,6]. In our calculation the Pb also appears as a rather good vibrator and the predicted effects on the energy shifts are consistent with the experiment. This is probably related to the fact that ^{208}Pb is a double-magic nucleus. It would be very important to study non-magic, open-shell or deformed nuclei which are expected to be poorer vibrators than double-magic nuclei. In particular, it is known that the energy of the GDR is strongly affected by the deformation, indicating a possible strong coupling between dipole and quadrupole degrees of freedom. This may induce a modification of the cross-section stronger than the predicted 10 % to 20% for spherical-magic nuclei. In this respect, extensions of the presented results to open shell and deformed nuclei are called for.

In conclusion, we would like to stress that in addition to the DGDR excitation several states are contributing to the cross-section in the DGDR energy region. When the non-linearities and the anharmonicities are taken into account the total theoretical cross-section above the IVGQR come rather close to the experimental result for the Coulomb excitation of Pb.

Acknowledgement

This work has been partially supported by the spanish DGICyT under contract PB92-0663, by the Spanish-Italian agreement between the DGICyT and the INFN and by the Spanish-French agreement between the DGICyT and the IN2P3.

7 Appendix

We just need to know

$$H_{\lambda\mu}(\beta, t) = \int_0^{+\infty} (e^{i\omega t}(-1)^{\lambda+\mu} + e^{-i\omega t})\omega^\lambda K_\mu(\beta\omega)d\omega \quad (41)$$

with $\mu \geq 0$, since $H_{\lambda\mu}(\beta, t) = H_{\lambda|\mu|}(\beta, t)$. Considering the cases $\lambda + \mu$ even or odd, together with t positive, negative or null, the integral (41) will be proportional to integrals in [24]. Combining all cases we get

$$\begin{aligned} H_{\lambda\mu}(\beta, t) = & \\ & (1 + (-1)^{\lambda+\mu}) \frac{2^{\lambda-1}}{\beta^{\lambda+1}} \Gamma\left(\frac{1+\lambda+\mu}{2}\right) \Gamma\left(\frac{1+\lambda-\mu}{2}\right) F\left(\frac{1+\lambda+\mu}{2}, \frac{1+\lambda-\mu}{2}; \frac{1}{2}; -\frac{t^2}{\beta^2}\right) - \\ & i (1 - (-1)^{\lambda+\mu}) \frac{2^\lambda t}{\beta^{\lambda+2}} \Gamma\left(\frac{2+\lambda+\mu}{2}\right) \Gamma\left(\frac{2+\lambda-\mu}{2}\right) F\left(\frac{2+\lambda+\mu}{2}, \frac{2+\lambda-\mu}{2}; \frac{3}{2}; -\frac{t^2}{\beta^2}\right) \end{aligned} \quad (42)$$

These hypergeometric functions can be transformed following [20] as

$$\begin{aligned} F\left(n + \frac{1}{2}, n + \frac{1}{2} - \mu; m + \frac{1}{2}; -x^2\right) = & \frac{1}{(1+x^2)^{2n-\mu-m+1/2}} \\ & \times F\left(m-n, m-n+\mu; m+\frac{1}{2}; -x^2\right) \end{aligned} \quad (43)$$

If $\lambda + \mu$ is even, then $m = 0$ and $n = \frac{\lambda+\mu}{2}$. Whereas if $\lambda + \mu$ is odd, then $m = 1$ and $n = \frac{\lambda+\mu+1}{2}$. Therefore, in the cases in which we are interested $m - n$ is an integer ≤ 0 , and the latter hypergeometric function reduces to the following polynomial

$$F(-\ell, b; c; z) = \sum_{k=0}^{\ell} \frac{(-\ell)_k (b)_k}{(c)_k} \frac{z^k}{k!} . \quad (44)$$

References

- [1] A. Bohr and B.R. Mottelson, Nuclear Structure, vol. II, (W.A. Benjamin, N.Y., 1975)
- [2] N. Frascaria, Nucl. Phys. A 282 (1988) 245c
- [3] S. Mordechai et al., Phys.Rev.Lett. 60(1988)408
- [4] R. Schmidt et al., Phys. Rev. Lett. 70 (1993) 1767

- [5] J. Ritman et al, Phys. Rev. Lett. 70 (1993) 533
- [6] J. Stroth et al, in the Proceedings of the "Groningen Conference on Giant Resonances", June 28-July 1, 1995, Nucl. Phys. A 599 (1996)307c; K. Boretzky et al., GSI preprint-96-27 to be published on Physics Letters B.
- [7] Ph. Chomaz and N. Francaria, Phys. Rep. 252 (1995) 5
- [8] K.Govaert et al., Phys. Lett. B335(1994)113
- [9] F. Catara, Ph. Chomaz and N. Van Giai, Phys. Lett. B 233 (1989) 6
- [10] D. Beaumel and Ph. Chomaz, Ann. Phys. (N.Y.) **213** (1992) 405.
- [11] C. A. Bertulani, L. F. Canto, M. S. Hussein and A. F. R. de Toledo Piza, Phys. Rev. C 53 (1996) 334
- [12] C. Volpe, F. Catara, Ph. Chomaz, M. V. Andrés and E. G. Lanza, Nucl. Phys. A 589 (1995) 521; Nucl. Phys. A 599 (1996) 347c.
- [13] P. Ring and P. Schuck, The nuclear many-body problem (Springer, Berlin, 1981)
- [14] F. Catara and U. Lombardo, Nucl. Phys. A 455 (1986) 158
- [15] F. Catara, Ph. Chomaz and A. Vitturi, Nucl. Phys. A 471 (1987) 661
- [16] F. Catara and Ph. Chomaz, Nucl. Phys. A 482 (1988) 271c
- [17] F. Catara, Ph. Chomaz and N. Van Giai, Phys. Lett. B277 (1992) 1
- [18] V.Yu.Ponomarev et al., Phys. Rev. Lett. 72 (1994) 1168
- [19] AA. Alder and K. Winther, Nucl. Phys. A319 (1979) 518
- [20] M. Abramowitz and I.A. Stegun, Handbook of mathematical functions (Dover publications, N.Y., 1965), p. 379 and 559
- [21] N. V. Giai, Suppl. Prog. Theor. Phys. 74-75 (1983) 330; N. V. Giai and H. Sagawa, Phys. Lett. B106 (1981) 379.
- [22] C. Benesh, B. Cook and J. Vary, Phys. Rev. C40 (1989) 1198.
- [23] C. A. Bertulani, V. Yu. Ponomarev and V. V. Voronov, preprint nucl-th/9606004 at preprint archive <http://xxx.lanl.gov/>
- [24] I.S. Gradshteyn and I.M. Ryzhik, Tables of integrals, series and products (Academic Press, N.Y., 1965).